

CHAPTER 6a

Human Liver and Neuronal Interactomes
Reveal Novel Binding Partners for the T3 Receptor
Isoform $\alpha 1$

Marcel E. Meima, **Karn Wejaphikul**, Selmar Leeuwenburgh,
Anja L.M. van Gucht, Lona Zeneyedpour, Lennard J.M. Dekker,
W. Edward Visser, Theo M. Luider, Robin P. Peeters

Submitted

<http://hdl.handle.net/1765/119488>

6

Abstract

Thyroid hormone receptors (TRs) recruit cofactor complexes to regulate their transcriptional activity. Mutations in the TR α 1 isoform result in a syndrome of resistance to thyroid hormone α (RTH α) that is characterized amongst others by growth retardation, and intellectual and motor disabilities. However, the severity of the phenotype differs widely between patients. To fully understand the impact of mutations in the RTH α syndrome beyond the effect on binding of T3 to TR α 1, a comprehensive elucidation of the profiles of TR α 1-associated cofactors in different tissues is required. In this study, we used a tandem-affinity purification method to identify TR α 1-interactomes from a liver cell model and a neuronal cell model in the presence or absence of the ligand T3. The interactomes differed extensively between liganded and unliganded receptors. However, they mostly overlapped between the different cell types, suggesting that the general regulatory mechanisms are rather conserved in different cells. The presence of known cofactors, such as NCoR1, SRC1 and the mediator complex confirmed the validity of the approach. In addition, we identified novel putative binding partners including transcription factors and chromatin remodelling proteins. We confirmed the findings by co-immunoprecipitations. The identification of these novel binding partners of TR α 1 expands the understanding of the molecular regulation of TR α 1 and allows subsequent studies on the mechanisms how specific TR α 1 mutations contribute to the RTH α phenotype.

Introduction

Thyroid hormone receptors (TRs) are ligand-dependent transcriptional regulators that are pivotal for the control of development, metabolism and tissue homeostasis (1,2). TRs are encoded by two genes (*THRA* and *THRB*) that yield three nuclear hormone-binding isoforms, TR α 1, TR β 1, and TR β 2, which have high homology but differ in their tissue-specific distribution. TRs predominantly bind as heterodimers with Retinoid X Receptors (RXR) to thyroid hormone response elements (TREs) to regulate the expression of target genes.

Mutations in TRs can cause syndromes of resistance to thyroid hormone (RTH) with distinct clinical outcomes. RTH α , caused by mutations in *THRA*, was recently identified and is characterized by intellectual disability, growth and psychomotor retardation, and developmental delay (3). The severity of the phenotype and the panel of traits differ widely between patients. Apart from ligand binding affinity, this may be explained by impaired recruitment of specific cofactors, some of which may be expressed or associated in a tissue-specific pattern. A thorough identification of tissue-specific interactomes of liganded and unliganded TR α 1 will therefore contribute to better understanding the molecular regulation of TR α 1 action in health and disease.

Similar to other nuclear receptors (NRs), TR activity is regulated via recruited cofactors that determine the local chromatin structure and thereby facilitate the accessibility to the promoter region of target genes (4). In the absence of triiodothyronine (T3), the biologically active form of thyroid hormone (TH), TRs are bound to members of the nuclear corepressor/silencing mediator for retinoid and thyroid hormone receptors (NCoR/SMRT) proteins that recruit a complex of proteins that favour histone deacetylation, which renders the local chromatin in a closed conformation. Binding of T3 induces conformational changes of the TRs that cause the NCoR/SMRT complex to dissociate and results in the recruitment of members of the Nuclear Coactivator (NCoA) family, also known as steroid receptor coactivators (SRCs), which are complexed with histone acetyl transferases (HATs). This results in acetylation of histones, which turns the local chromatin in an open and accessible state allowing the subsequent recruitment of the Mediator complex, which recruits general transcription factors (GTFs) and the RNA polymerase II complex to initiate gene transcription (5-7). Apart from these classical cofactors, numerous proteins have been identified that can directly bind to TRs and modulate their transcriptional activity, including other scaffolding and chromatin remodeling proteins, transcription factors, signaling proteins, and structural proteins (8-11). Some of these non-classical cofactors exhibit isoform preference, (11,12), adding to the complexity of TH action.

Previous studies that identified TR-interacting proteins and protein complexes used two-hybrid (8), GST-pull downs (11), and affinity purification methods (5,12). Fozzatti and coworkers developed a tandem-affinity purification (TAP) method to purify isoform-specific interacting proteins from HeLa cells (12). However, their study was limited to proteins associated

with TR mutants deficient in T3-binding and returned only a limited number of proteins that were isolated from SDS-PAGE gels. In the current study, we optimized their method to purify TR α 1-interactomes from models for liver cells and neuronal cells in the presence or absence of ligand, and subsequently to co-purify proteins of the intact complexes that were identified by LC-MS/MS without prior separation. The interactomes mostly overlapped between the two cell types, but differed strongly between liganded and unliganded receptors. Importantly, we identified novel interacting proteins and multisubunit complexes with yet to be identified regulatory functions in TH action.

Materials and methods

Cell culture

293FT (Thermofisher, #R70007), human HepG2 (ATCC[®] HB-8065[™]) hepatocellular carcinoma and human SH-SY5Y (ATCC[®] CRL-2266[™]) neuroblastoma cells were grown in DMEM/F12 medium (Lonza), supplemented with 9% FBS (Lonza), 100 U/ml penicillin, 100 μ g/ml streptomycin (Lonza), and 100 nM Na₂SeO₃ at 37 °C and 5% CO₂. Cells were routinely passaged and medium refreshed twice a week. Before transfections, the medium was first replaced with hypothyroid Ct-medium (DMEM/F12, 9% charcoal-treated FBS without penicillin/streptomycin).

Constructs

The plasmid pCDNA3-FLAGTR α 1 was used to transiently express FLAG-tagged human TR α 1 as described previously (13). A lentiviral construct was used to stably express N-terminal FLAG and hemagglutinin (HA) double-epitope tagged human TR α 1 (from hereon called FHTR α 1). To select cells, we used a construct that produces a bicistronic messenger from which FHTR α 1 is translated together with the puromycin selection marker coupled to GFP by a cleavable 2A peptide (Supplementary Figure S1). The entry vectors pENTL1-MCS-R5, pENTL5-IRESpuro2AGFP-R2, the lentiviral vector pWCAGpCasC, and the packaging vectors pMD2.G and psPAX2 were all kindly gifted by Dr. Lammert Dorssers (Department of Pathology, Erasmus MC, Rotterdam). Please see the supplemental methods for the generation of the plasmids pWCAGpCasC-MCS-IRESpuro2AGFP and pWCAGpCasC-FHTR α 1-IRESpuro2AGFP (from hereon called pLentiMCS or pLentiFHTR α 1) (14).

Lentivirus production and transduction

To generate lentiviral particles, 293FT cells were seeded into 10 cm dishes and transfected with 4 μ g of pLentiMCS or pLentiFHTR α 1, 4 μ g psPAX2, and 4 μ g pMD2.G at ~90% confluency in growth medium without antibiotics, using Xtreme Gene. Supernatants were harvested at 48 and 72 hour after transfection and subsequently, filtered through 0.45 μ m

PES filters to obtain cell-free lentiviral stocks. For infections, HepG2 and SH-SY5Y cells were seeded in growth medium in 6-wells dishes and infected at ~25% confluency with different amounts of viral stocks. After 2 days, infected cells were selected with 2 μ g/ml puromycin. The medium was refreshed every 2-3 day and wells with similar number of puromycin resistant cells were expanded and used for further analysis.

Luciferase assay

HepG2 and SH-SY5Y cells stably expressing FHTR α 1 were seeded in 24 wells plates and grown in growth medium to 70-80% confluency. The cells were transfected with Xtreme Gene (Roche) using the manufacturer's protocol in Ct medium with 200 ng of the plasmid pdV-L1 that contains firefly luciferase under control of a direct and inverted repeat TRE, and renilla luciferase as described previously (15). Results are presented as the means \pm SEM of three experiments performed in triplicate.

Tandem-affinity purification (TAP)

FHTR α 1 expressing or MCS control cells were seeded in growth medium in 10 (HepG2) or 20 (SH-SY5Y) 145 mm dishes per cell line per condition. At 80-90% confluency, the cells were incubated overnight with DMEM/F12 supplemented with 0.1% BSA and subsequently incubated for 4 hours with vehicle or 100 nM T3. FHTR α 1-containing protein complexes in nuclear extracts were sequentially purified on anti-FLAG and anti-HA resins as described previously with adaptations (12). A detailed protocol of the purification and LC-MS/MS analysis of the enriched proteins is provided in the supplementary material section (14).

Co-immunoprecipitations

HepG2 or SH-SY5Y cells were transfected with the plasmids pCDNA3-FLAGTR α 1 or pCDNA3 as empty vector control in Ct medium with Xtreme Gene (Roche) according to the manufacturer's protocol. After overnight incubation in DMEM/F12 supplemented with 0.1% BSA, the cells were stimulated with vehicle or 100 nM T3 for 4 hours. Cells were collected in buffer A (10 mM Hepes.NaOH, 10 mM KCl, 0.1 mM EDTA, 1 mM DTT, cOmplete™ protease inhibitors (Roche), pH 7.9) and lysed by adding 0.6% NP40. Nuclei were extracted in buffer C (20 mM HEPES.NaOH, 400 mM NaCl, 1 mM EDTA, 1 mM DTT, cOmplete™ protease inhibitors, pH 7.9) and diluted in buffer D (20 mM HEPES.NaOH, 1 mM EDTA, cOmplete™ protease inhibitors, pH 7.9) to restore NaCl concentrations to 150 mM. Nuclear extracts were incubated overnight with 10 μ l bed volume of FLAG-agarose beads (clone M2; Sigma). The beads were washed 4 times with 1 ml wash buffer (20 mM HEPES.NaOH, 150 mM NaCl, 1 mM EDTA, 1 mM DTT, pH 7.9) and eluted with 200 μ g/ml FLAG peptide in wash buffer. Nuclear extracts and immunocomplexes were denatured in 1x NuPAGE LDS sample buffer supplemented with 10 mM DTT at 70 °C for 10 minutes.

Immunoblotting

Nuclear extracts and immunocomplexes were separated on 4-15% Mini-Protean TGX gels (Bio-rad) and transferred to Immobilon PDVF membranes (Whatmann). Membranes were probed with 1:1000 dilutions (unless stated otherwise) of the following antibodies: FLAG M2 clone (F1804, RRID:AB_262044), Prox1 (1:2000) (P7124, RRID:AB_1079691) (both Sigma Aldrich), HA (clone C29F4, #3724, RRID:AB_10693385), CHD4 (clone D8B12, #11912, RRID:AB_2751014), NCoR1 (#5948, RRID:AB_10834809), RXR α (clone D6H10, #3085, RRID:AB_11140620), SRC-1 (clone 128E7, #2191, RRID:AB_2196189), HDAC3 (clone 7G6C5, #3949, RRID:AB_10986336), MED26 (clone D4B1X, #14950, RRID:AB_2798656), Histone 3 (clone 1B1B2, #14269, RRID:AB_2756816), Brg1 (clone D1Q7F, #49360, RRID:AB_2728743), KIF11/Eg5 (#7625, RRID:AB_10860412) (all Cell Signaling Technology). Blots were then probed with 1:3000 dilutions of horse radish peroxidase (HRP)-conjugated goat anti-mouse or goat anti-rabbit (Biorad) and proteins were visualized by Enhanced Chemiluminescence (ECL).

Results

Stable expression of FHTR α 1 in HepG2 and SH-SY5Y cells

HepG2 and SH-SY5Y cell lines that stably expressed FHTR α 1 transcribed from a bicistronic messenger RNA that also encodes the puromycin selection marker and GFP for selection of transduced cells (Supplementary Figure S1 (14)) were successfully generated. Cells transduced with the empty vector (MCS) that only expresses the puromycin selection marker and GFP were also generated as a control. Equal amounts of nuclear extracts prepared from all stable cell lines were analysed by immunoblotting. By probing with HA antibodies, specific bands at the predicted size of ~49 kD were visualized for both HepG2 and SH-SY5Y cells (Figure 1A). A dose-dependent increase in luciferase activity was found in both HepG2 and SH-SY5Y cells expressing FHTR α 1 after 24 hours T3 incubation, confirming that the FH-tag did not interfere with receptor activation (Figure 1B).

Tandem-affinity purifications (TAP)

To confirm the effectiveness of our TAP protocol, we first purified FHTR α 1 from HepG2 cells that had been stimulated for 4 hours with 100 nM T3 or vehicle. A third of the final eluate was separated by SDS-PAGE. After visualization by Colloidal Coomassie Blue staining, the bait as well as additional bands were shown in lanes with eluates from HepG2/FHTR α 1 but not control (MCS) cells, confirming that our method is effective to purify TR α 1 and associated proteins (Supplementary Figure S2 (14)). In addition, the staining pattern differed between cells incubated in the presence or absence of T3, indicating that the association of many proteins depended on the occupation state of the receptor.

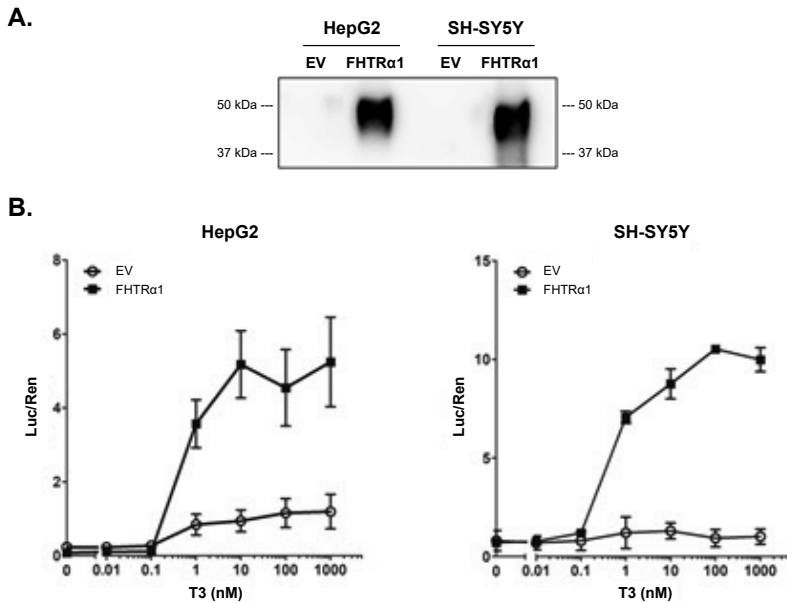


Figure 1. *FHTRα1* has T3-stimulated activity. (A) Western blot showing expression of FHTRα1 in HepG2 and SH-SY5Y cells. Equal amounts of nuclear proteins extracted from HepG2 and SH-SY5Y cells with stable integration of FHTRα1 or empty vector (MCS) as control were immunoblotted with an HA antibody. (B) Luciferase reporter assay showing T3-dependent transcriptional activity of FHTRα1. HepG2 and SH-SY5Y cells with stable integration of FHTRα1 or empty vector (MCS) as control were transfected with a reporter construct in which the gene encoding firefly luciferase is under control of a TRE and constitutively expresses renilla luciferase as transfection control, incubated with increasing concentrations of T3 and lysates measured for luciferase and renilla activity. Data represent mean \pm SEM of three independent experiments performed in triplicate.

General composition of the interactomes

An additional purification from HepG2 cells, and two independent purifications from SH-SY5Y cells were performed, and all eluates were subjected to LC-MS/MS analysis. Proteins that were identified with an FDR of 1% in any of the control purifications were excluded. A total number of 252 proteins were identified in all purifications combined (Supplementary Table 1 (14)). Gene enrichment analysis for cellular compartments using DAVID showed that 148 were nuclear proteins (Benjamini corrected p value for enrichment 2.0×10^{-20} , Supplementary Figure S3 (14)). Proteins generally overlapped between purifications for the same cell type and condition (Table 1), although the second HepG2 purification returned a larger number of hits many of which were not present in the first purification. This may be due to impurity of the enriched complex, which is underscored by the relatively large number of ribosomal and ribonuclear proteins (Table 2, Supplementary Table 1 (14)).

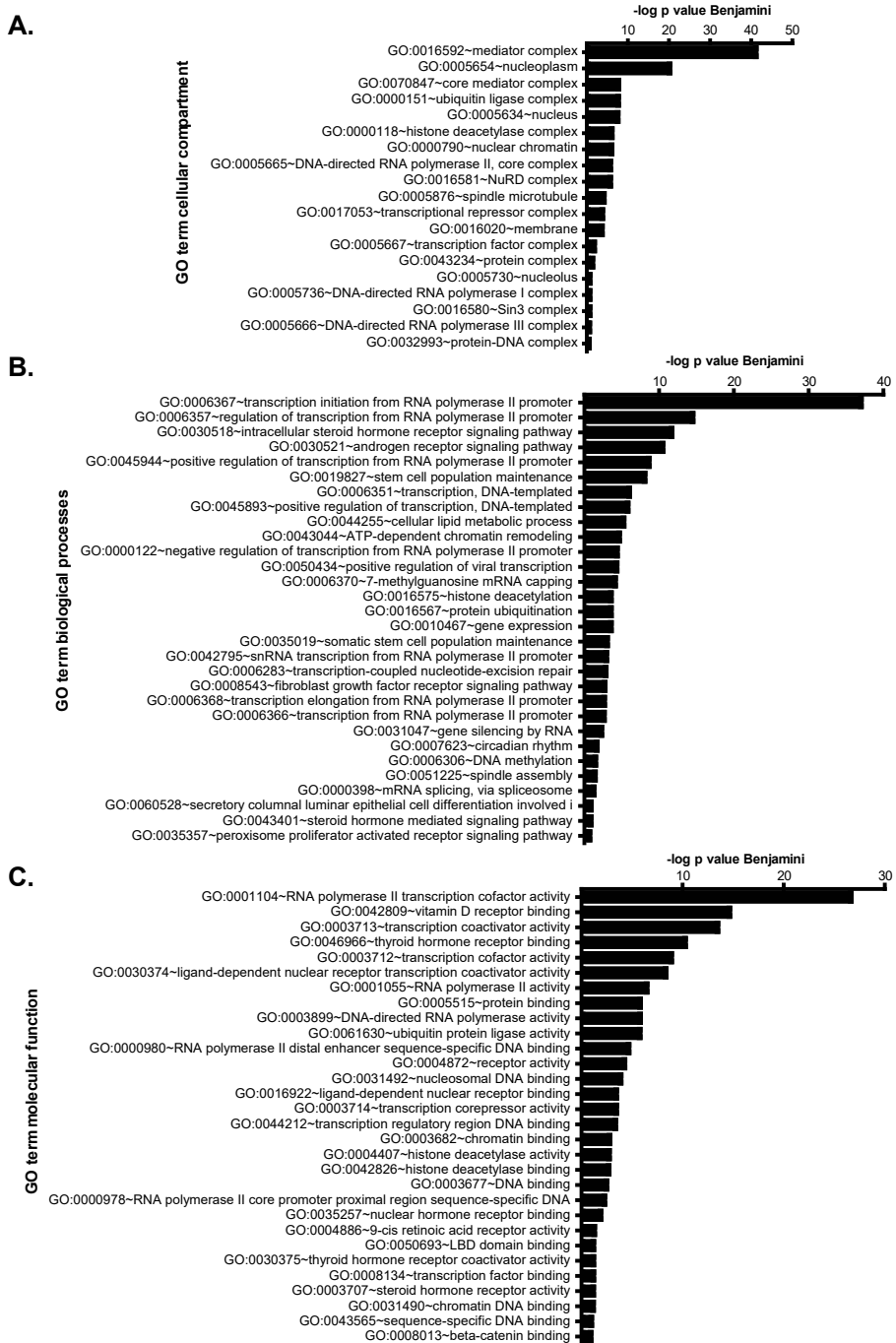


Figure 2. Enrichment of GO terms in the profile. Proteins that were replicated in for at least one cell line and condition (see Table 2) were analysed for enrichment of (A) cellular compartments, (B) biological processes or (C) molecular function using DAVID (minimum count 2, ease 0.1). The top 30 most significant GO terms are displayed. P values were adjusted for false discovery rates using the Benjamini correction.

Table 1: Total number of hits and replication between purifications

Cell/condition	Purification 1	Purification 2	Overlap
HepG2 vehicle	22	130	11
HepG2 T3	58	76	37
SH-SY5Y vehicle	21	21	9
SH-SY5Y T3	20	65	14

Proteins and peptides were compared with Scaffold version 4.8.3. FDR was set at 1% for proteins and peptides. Probability scores that met criteria were 5% for proteins and 78% for peptides and 2 peptides minimum for HepG2 purification and 99% and 91% with 1 peptide for the other purifications. Proteins found in control purifications were excluded.

Many copurifying proteins belong to protein complexes and are involved in gene regulation

Of the total number of proteins, 55 were replicated for at least one cell type plus condition, and are listed with probability scores and coverage (exclusive unique peptides and percentage coverage) in Table 2. For global analysis of the functional relevance of these proteins, we used DAVID for gene enrichment analysis (Figure 2). For biological processes and molecular functions, we found enrichment of transcriptional regulation via the RNA polymerase II complex, nuclear receptor signalling and regulation, histone modification, chromatin remodelling and cofactor binding, all confirming a strong association of the profile with gene regulation. Enrichment for cellular components showed that the profile is strongly enriched for nuclear chromatin binding proteins and/or proteins associated with complexes that are involved in gene regulation, such as Mediator complex, histone deacetylation complexes, RNA polymerase II complex, and the nuclear remodelling and deacetylase (NuRD) complex. Screening of the entire profile of 252 proteins for cellular components identified enrichment of additional chromatin remodelling complexes with lower coverage and significance, including the strongly overlapping SWItch/Sucrose Non-Fermentable (SWI/SNF), neuron-specific BRG1 or HBRM-associated factor (nBAF) and neural progenitor BAF (npBAF) complex, and the mixed-lineage leukemia 4 (MLL4) complex (Supplementary Figure S3 (14)).

Dependence of ligand state and cell lineage on composition of TRα1-interactomes

To characterize the protein complexes in our profiles and the effect of T3-binding, we built an interaction network based on experimentally proven interactions using the STRING database where we separated between proteins found in the presence or absence of T3 (Figure 3). In addition, we listed proteins by complexes and/or function by cell-type and ligand

state (Table 3). Since there were differences in recovery between HepG2 and SH-SY5Y cells and because distant interactions of some members of the complexes may have been so weak that they were close to the limit of detection, we included here proteins that were found in a single purification, when they belonged to a specific protein complex. As expected, TR α 1 is associated with RXRs in the presence or absence of T3. In the absence of T3, the receptor is associated with the NCoR1-complex that further contains HDAC3 and the F-Box/WD40 repeat-containing proteins TBL1X and TBL1XR1. Both the corepressor nuclear receptor interacting protein 1 (NRIP1) and the Mediator complex were found under both conditions but strongly upregulated by T3, as indicated by the higher number of peptides and number of subunits for Mediator in the presence of T3, whereas the RNA polymerase II complex was only found in the presence of T3 (Figure 3 and Table 2). Surprisingly, we only found NCoAs in a single purification in the presence of T3 from HepG2, namely NCoA1/SRC1 and NCoA3/SRC3 (Supplementary Table 1 (14)), and no HATs. The NuRD complex was also present under both conditions, but slightly enriched by T3 (Table 3). Like NRIP1, the association of prospero homeobox 1 (Prox1) was increased by T3, whereas the phosphoserine/threonine phosphatase PPM1G was only found in the absence of T3.

The profiles extensively overlapped between cell lines. Both HepG2 and SH-SY5Y cells yielded the NCoR/SMRT, Mediator, and NuRD complexes (Tables 2 and 3). A number of hits appeared specific for a single cell line. NRIP1 was abundantly present in purifications from T3-treated HepG2 cells only (Table 2). In SH-SY5Y cells, we found a higher number of SWI/SNF complex members and specific association of transcription factor 4 (TCF4), and the protein encoded by the open reading frame C11orf84 (Table 3). In addition, the structural proteins KIF11 (also known as thyroid hormone receptor interacting protein 5 (TRIP5) and Eg5) and CLASP2 were only found in from SH-SY5Y cells. Other proteins that copurified with FHTR α 1 in a cell-type specific manner appear less relevant for gene regulation, such as extracellular proteins, mitochondrial enzymes or membrane transport.

Co-immunoprecipitations confirm LC-MS/MS profiles

To validate selected hits from our profiles, we immunoprecipitated FLAG-TR α 1 from transiently transfected HepG2 and SH-SY5Y cells using FLAG antibodies and immunoblotted the immunocomplexes (Figure 4). In both cell types, NCoR1 and HDAC3 were only detected in cells treated with vehicle, and SRC1 and MED26 (as representative of the Mediator complex) in T3-treated cells, whereas the association of RXR α was modestly increased by T3. Chromodomain helicase 4 (CHD4) was chosen as representative of the NuRD complex and specifically copurified with FLAG-TR α 1 from both cell types. The transcription Prox1 copurified with FLAG-TR α 1 from both cell types as well, and the association was strongly increased by T3, consistent with the increased coverage of Prox1 with T3 in the LC-MS/MS profiles (Table 2). Only BRG1 (also known as SMARCA4 and belonging to SWI/SNF and BAF complexes) and KIF11 were also present in immunoprecipitations from cells transfected with the empty vector and thus are likely false positives (results not shown).

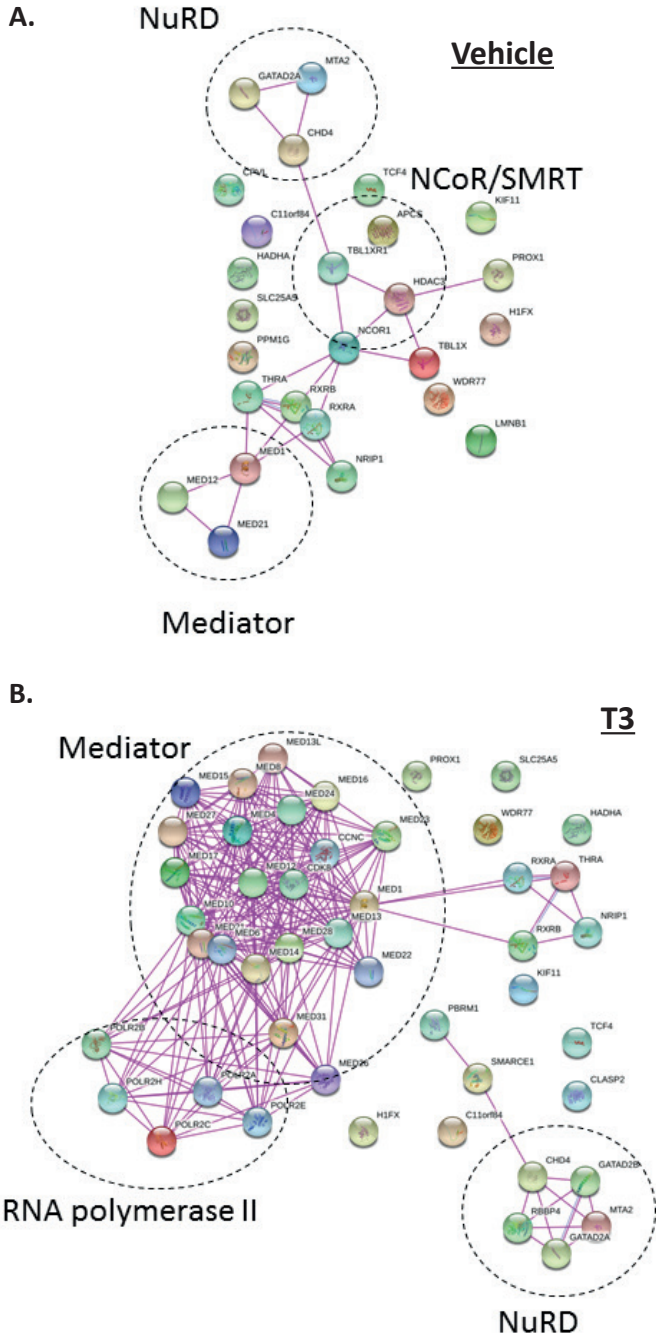


Figure 3. Protein networks in the protein profile and the effect of ligand state. Proteins that were replicated in at least one cell line and condition (see Table 2) were mined for existing experiment-based protein interactions, using STRINGS with minimum required interaction scores set at medium (0.400). Profiles found for the (A) absence or (B) presence of T3 were analysed separately. Dashed circles indicate protein complexes.

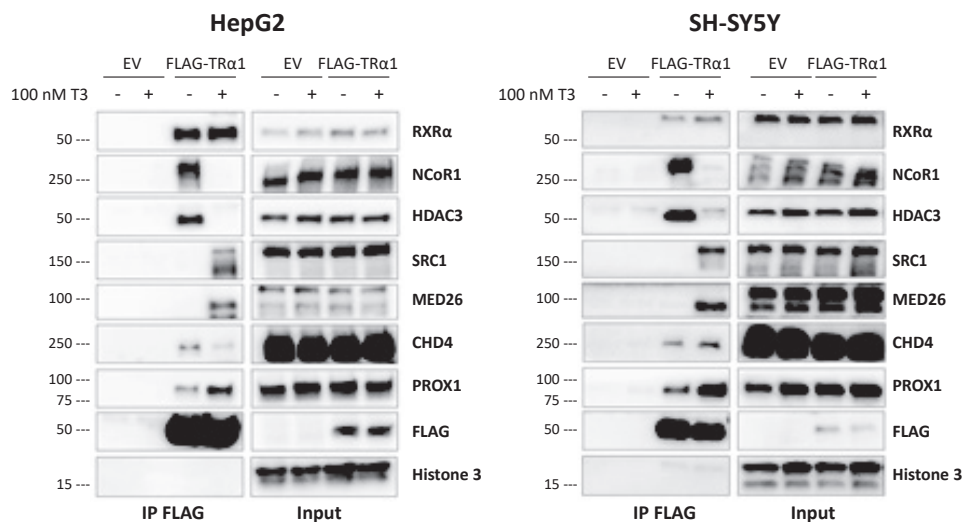


Figure 4. Immunoprecipitation confirms association of selected proteins from the profiles with FHTRα1. Representative immunoblots showing co-immunoprecipitation of selected hits with FHTRα1 from HepG2 and SH-SY5Y cells. Nuclear extracts from HepG2 and SH-SY5Y cells transfected with FLAG-TRα1 or empty vector (EV) as control were subjected to immunoprecipitation with anti-FLAG resin, proteins eluted with the FLAG peptide and the immunocomplexes or 10% of the nuclear extracts as input control subjected to western blotting. Segments of the blot around the expected molecular weight of the targeted proteins were immunoblotted with the indicated antibodies. Histone 3 was used as control for equal input.

Table 2. Protein replicated for at least one cell type and condition (**MW**, molecular weight; **Prob.** probability; **EUP**, exclusive unique peptides; **Cov.** coverage)

Protein name	Gene ID	MW (kDa)	HepG2						SH-SY5Y										
			Vehicle			100 mM T3			Vehicle			100 mM T3							
			Prob (%)	# EUP	Cov (%)	Prob (%)	# EUP	Cov (%)	Prob (%)	# EUP	Cov (%)	Prob (%)	# EUP	Cov (%)					
Serum amyloid P-component	APCS	25.4																	
Uncharacterized protein C11orf84	C11orf84	41.0																	
Cyclin-C	CCNC	33.2																	
Cyclin-dependent kinase 8	CDK8	53.3				100	3	9.9	100	1	3.5								
Chromodomain-helicase-DNA-binding protein 4	CHD4	218.0				100	5	10.1	100	2	4.5								
CLIP-associated protein 2	CLASP2	141.1				100	2	1.2	100	1	0.7								
Probable serine carboxypeptidase CPVL	CPVL	54.2				100	2	3.8	99.9	1	2.1								
Transcriptional repressor p66-alpha	GATAD2A	68.1				100	2	5.7	99.9	1	1.9								
Transcriptional repressor p66-beta	GATAD2B	65.3				100	2	6.8	100	3	10.0								
Histone H1x	H1FX	22.5				100	2	3.9	100	4	6.2								
Trifunctional enzyme subunit alpha, mitochondrial	HADHA	83.0				100	7	23.6	100	4	9.6								
Histone deacetylase 3	HDAC3	48.8				100	1	3.2	99.8	1	4.1								
Kinesin-like protein KIF11	KIF11	119.2				99.6	1	91.6	100	21	16.3								
Lamin-B1	LMNB1	66.4				99.9	1	0.9	100	17	13.4								
Mediator of RNA polymerase II transcription subunit 1	MED1	168.5				99.7	1	5.4	99.6	1	5.4								
						99.3	1	2.4	100	1	2.4								

Protein name	Gene ID	MW (kDa)	HepG2						SH-SY5Y									
			Vehicle			100 nM T3			Vehicle			100 nM T3						
			Purification 1 Prob (%)	# EUP	Cov (%)	Purification 2 Prob (%)	# EUP	Cov (%)	Purification 1 Prob (%)	# EUP	Cov (%)	Purification 2 Prob (%)	# EUP	Cov (%)	Purification 1 Prob (%)	# EUP	Cov (%)	
Mediator of RNA polymerase II transcription subunit 10	MED10	15.7				100	4	36.3	100	1	6.7							
Mediator of RNA polymerase II transcription subunit 12	MED12	243.1		99.7	1	0.6	100	19	11.8	100	8	4.9				100	3	1.8
Mediator of RNA polymerase II transcription subunit 13	MED13	239.3				100	17	10.2	100	6	3.9							
Mediator of RNA polymerase II transcription subunit 13-like	MED13L	242.6				100	5	2.9	100	3	2.5							
Mediator of RNA polymerase II transcription subunit 14	MED14	160.6				100	16	12.7	100	7	5.2					100	3	2.4
Mediator of RNA polymerase II transcription subunit 15	MED15	86.8				100	5	8.3	100	2	3.1					99.6	1	1.4
Mediator of RNA polymerase II transcription subunit 16	MED16	96.8				100	8	10.4	100	2	2.4					99.8	1	1.3
Mediator of RNA polymerase II transcription subunit 17	MED17	72.9				100	14	19.7	100	7	10.6					100	2	3.7
Mediator of RNA polymerase II transcription subunit 21	MED21	15.6				100	2	22.2	100	2	22.2							
Mediator of RNA polymerase II transcription subunit 22	MED22	22.2				100	6	21.0	100	3	13.5							
Mediator of RNA polymerase II transcription subunit 23	MED23	156.5				100	6	4.5	99.9	1	1.2							
Mediator of RNA polymerase II transcription subunit 24	MED24	110.3				100	9	13.1	100	4	5.3					100	1	1.8

Protein name	Gene ID	MW (kDa)	HepG2						SH-SY5Y																	
			Vehicle			100 nM T3			Vehicle			100 nM T3														
			Prob (%)	# EUP	Cov (%)	Prob (%)	# EUP	Cov (%)	Prob (%)	# EUP	Cov (%)	Prob (%)	# EUP	Cov (%)												
Mediator of RNA polymerase II transcription subunit 26	MED26	65.4	100	5	8.2	100	4	7.0																		
Mediator of RNA polymerase II transcription subunit 27	MED27	35.4	100	7	25.1	100	2	6.4																		
Mediator of RNA polymerase II transcription subunit 28	MED28	19.5	100	4	20.8	100	1	7.3									99.6	1	7.3							
Mediator of RNA polymerase II transcription subunit 31	MED31	15.8	100	3	19.1	100	1	13.0																		
Mediator of RNA polymerase II transcription subunit 4	MED4	29.7	100	8	37.8	100	5	22.2																		
Mediator of RNA polymerase II transcription subunit 6	MED6	28.4	100	8	24.0	100	5	24.4									98.9	1	4.5	100	1	5.7				
Mediator of RNA polymerase II transcription subunit 8	MED8	29.1	100	5	22.8	100	4	16.8																		
Melanosis-associated protein MTA2	MTA2	75.0	100	3	6.1	100	4	7.2																		
Nuclear receptor corepressor 1	NCOR1	270.2	100	37	19.5	100	36	15.9																		
Nuclear receptor-interacting protein 1	NRIP1	126.9	100	5	5.8	100	22	22.9																		
Protein polybromo-1	PBRM1	193.0																								
DNA-directed RNA polymerase II subunit RPB1	POLR2A	217.2	100	22	13.3	100	7	4.7																		
DNA-directed RNA polymerase II subunit RPB2	POLR2B	133.9	100	12	12.2	100	2	2.1																		

Protein name	Gene ID	MW (kDa)	HepG2						SH-SY5Y											
			Vehicle			100 nM T3			Vehicle			100 nM T3								
			Purification 1 Prob (%)	# EUP	Cov (%)	Purification 2 Prob (%)	# EUP	Cov (%)	Purification 1 Prob (%)	# EUP	Cov (%)	Purification 2 Prob (%)	# EUP	Cov (%)	Purification 1 Prob (%)	# EUP	Cov (%)			
DNA-directed RNA polymerase II subunit RPB3	POLR2C	31.4	100	6	36	100	2	6.6	100	4	6.2	100	4	10.8	100	7	11.1	100	14	19.1
DNA-directed RNA polymerase I, II, III subunit RPABC1	POLR2E	24.6	100	4	23.8	100	2	8.6	100	2	4.5	100	3	6.1	100	3	9.2	100	4	9.2
DNA-directed RNA polymerase I, II, III subunit RPABC3	POLR2H	17.1	100	2	10.7	100	3	25.3	100	2	6.2	100	4	10.8	100	7	11.1	100	14	19.1
Protein phosphatase 1G	PPM1G	59.3	100	4	10.8	100	13	19.0	100	2	4.5	100	3	6.1	100	7	11.1	100	14	19.1
Prospero homeobox protein 1	PROX1	83.2	100	6	9.8	100	11	15.6	100	1	7.5	100	2	4.7	100	3	9.2	100	4	9.2
Histone-binding protein RBBP4	RBBP4	47.7	100	1	7.5	100	2	4.7	100	5	22.5	99.9	1	10.6	100	3	9.2	100	4	9.2
Retinoic acid receptor RXR-alpha	RXRA	50.8	100	5	18.6	100	4	22.9	100	7	26.1	100	7	26.1	100	3	9.2	100	4	9.2
Retinoic acid receptor RXR-beta	RXRB	56.9	100	10	30.0	100	6	23.5	100	12	41.7	100	7	26.1	100	3	9.2	100	4	9.2
ADP/ATP translocase 2	SLC25A5	32.9	100	2	7.4	100	2	7.1	99.7	1	3.7	99.7	1	3.7	100	2	6.3	100	3	9.3
SWI/SNF-related regulator of chromatin subfamily E member 1	SMARCE1	46.6																		
F-box-like/WD repeat-containing protein TBL1X	TBL1X	62.5	100	8	28.9	100	3	14.2												
F-box-like/WD repeat-containing protein TBL1XR1	TBL1XR1	55.6	100	13	48.4	100	6	19.8	100	3	9.7	100	4	12.5	100	2	6.3	100	3	9.3
Transcription factor 4	TCF4	71.3							100	1	1.4	100	1	1.4	100	2	3.8	100	2	3.8

Table 3: Proteins by complexes and/or molecular function

Complex	HepG2		SH-SY5Y	
	vehicle	T3	vehicle	T3
Nuclear receptors	THRA, RXRA, RXRB	THRA, RXRA, RXRB	THRA, RXRB	THRA, RXRB
NCoR/SMRT	NCoR1, NCoR2, HDAC3, TBL1X, TBL1XR1, TBL1Y		NCoR1, TBL1XR1	
Other corepressors	NRIP1	NRIP1	C11orf84	C11orf84
Mediator	MED1, MED12, MED21	MED1, MED4, MED6, MED7, MED8, MED9, MED10, MED11, MED12-17, MED13L, MED19-20, MED21-24, MED26-28, MED29, MED31, CCNC, CDK8		MED1, MED6, MED12, MED14-17, MED24, MED28
RNA polymerase II		POLR2A-C, POLR2D, POLR2E, POLR2H, POLR2I, PAF1, RECQL5, RPAP2		
NuRD	CHD4, MTA1, MTA2	CHD4, GATAD2A, GATAD2B, HDAC2, MBD3, MTA1, MTA2, MTA3, RBBP4, RBBP7		GATAD2B, HDAC2, MTA1, MTA2 , RBBP4
SWI/SNF nBAF npBAF	SMARCC2	SMARCB1		ACTL6A, PBRM1 , SMARCA4/ BRG1, SMARCB1, SMARCE1
Histones			H1FX	H1FX
Transcription factor	PROX1	PROX1	PROX1, TCF4	PROX1, TCF4
Phosphatases	PPM1G		PPM1G	
Methylosome complex	WDR77		WDR77	WDR77
Membrane transport	SLC25A5	SLC25A5		
Enzyme	HADHA, CPVL	HADHA	CPVL	
Structural	LMNB1		KIF11	CLASP2, KIF11
Extracellular			APCS	

Proteins that were replicated for a cell line and condition are in bold. Proteins that were not replicated were included when they were replicated for another cell line and condition or when they belong to a protein complex (normal font).

Discussion

In this study, we purified TR α 1 from two cell models in the presence and absence of the natural ligand T3 and identified several unknown binding partners of TR α 1 by LC-MS/MS. Our approach revealed that the composition of TR α 1-interactomes mostly overlaps between the two studied cell-types and strongly depends on ligand-state. In addition, we found novel putative binding partners, most notably transcription factors and proteins belonging to chromatin remodelling complexes.

Two important aims of our approach were to determine the effect of ligand and cell background on the composition of TR α 1-interactomes. As expected, the interactomes varied clearly between unliganded and liganded receptors. This was confirmed by co-immunoprecipitations for members of the NCoR1, NCoA/SRCs and Mediator complexes, but also for potentially novel candidates such as the transcription factor Prox1. Whether these novel partners act as global regulators of T3-dependent TR activity or are involved in the regulation of a subset of genes at the cross-road of TH and other signalling pathways remains to be elucidated. The analysis of cell specificity dependence was complicated by the fact that recoveries of the bait and number of co-purifying proteins were consistently lower from SH-SY5Y cells than from HepG2 cells. As a result, interactions that are weakly preserved or are only incorporated in a subset of transcriptional complexes could have fallen below the detection limit in purifications from SH-SY5Y cells. This is underscored by the recovery of substantially less members of conserved protein complexes like Mediator from SH-SY5Y cells than from HepG2 cells. The lower recovery is likely due to the lower amount of input from SH-SY5Y cultures, even though we used twice the amount of tissue culture plates. Despite this, a number of hits were replicated in a single type, for example NRIP1 in HepG2 cells and TCF4 in SH-SY5Y cells, suggesting a cell-type specific association with TR α 1 which could contribute to cell-type specific gene regulation. However, since according to the human protein atlas (<https://proteinatlas.org>) both proteins are expressed in liver and brain, but NRIP1 only in HepG2 and TCF4 only in SH-SY5Y cells, it cannot be proven whether the association is specific for the cellular context or merely a consequence of expression in the cell models.

Several proteins in our profiles belong to multisubunit chromatin remodelling complexes. Chromatin remodelling complexes combine different enzymatic activities that alter the local chromatin architecture by affecting the state of histone acetylation and methylation and repositioning nucleosomes. Most notably, we found many members of the NuRD complex, including CHD4, GATA zinc finger domain containing 2A and 2B (GATAD2A/GATAD2B), metastasis-associated factors (MTA1/MAT2/MTA3), histone binding proteins (RBBP4 and weakly RBBP7) and methyl-CpG domain binding protein (MBD3). The NuRD complex is a chromatin remodelling complex that facilitates predominantly transcriptional repression by combining helicase and histone deacetylase activities (16) and has been shown to repress TR activity in a *Xenopus* oocyte model (17). CHD4 was previously shown to co-purify with mutant TRs (12), and here co-immunoprecipitated with WT TR α 1 in HepG2 and SH-SY5Y

cells (Figure 4). Interestingly, CHD4 directly binds to the nuclear receptor Retinoid Orphan Receptor gamma (ROR γ) and inhibits its transcriptional activity (18).

Members of SWI/SNF complexes, also known as the BAF (BRG1/BRM-associated factors) complex, were weakly present in our profiles. BAF complexes are ATP-dependent chromatin remodelling complexes that confer epigenetic regulation of gene expression by altering the positioning of nucleosomes, and altered activity is associated with developmental disorders and cancer (19,20). Studies using TR β 1 and reporter construct injected *Xenopus* oocytes showed T3-stimulated recruitment of BRG1/SMARCA4 to chromatin (21). BAF proteins were predominantly found in SH-SY5Y cells treated with T3, but also in HepG2 cells treated with vehicle. However, immunoblotting against BRG1/SMARCA4 showed the presence of BRG1 in immunocomplexes of both control and FLAG-TR α 1 transfected HepG2 and SH-SY5Y cells, leaving a TR α 1-specific interaction questionable (results not shown). A third chromatin remodelling complex, the mixed-lineage leukemia 4 (MLL4) complex, was found in a single purification from HepG2 cells, and represented by the methylosome protein 50 (WDR5) in vehicle and T3-treated cells, and the histone lysine N-methyltransferase MLL4/KMT2D (sometimes also addressed as MLL2) and the lysine-specific histone demethylase UTX/KDM6A in T3-treated cells only. Mutations in MLL4/KMT2D and UTX/KDM6A cause the Kabuki syndrome, which is characterized by intellectual disability and distinct facial characteristics (22).

One of the strongest hits in our profiles was Prospero homeobox 1 (Prox1). Prox1 was associated with TR α 1 in both HepG2 and SH-SY5Y cells and binding was enhanced by the presence of T3, as indicated by the higher coverage and confirmed by co-immunoprecipitation (Figure 4). Prox1 is a transcription factor that has important functions in cell fate specification and metabolism (23-25). Prox1 interacts with several other NRs, such as COUP-TFII in lymphatic endothelial cells, and hepatic nuclear factor 4 (HNF4 α), liver receptor homologue-1 (LRH-1) and Retinoid Orphan Receptor (ROR) α and γ in liver (26-29). A recent systematic study of *in vitro* binding of peptides from coregulators to NRs showed that the Prox1 peptide bound to nearly all of the 24 NRs tested, including both TRs, which indicates that Prox1 may well be a general cofactor for NRs (30). In liver, Prox1 inhibits reverse cholesterol transport and represses HNF4 α and LRH-1 mediated expression of CYP7A1, an important enzyme for the conversion of cholesterol into bile acid (25,27,28,31), processes that are also regulated by TH (32).

The advantage of the TAP-purification method used is that the bait is incorporated into the protein complexes in the intact cell and purified under native condition. This approach therefore preserves the natural composition of the complexes. In addition, the two consecutive purification steps ensured recovery of highly pure complexes with limited background. We adopted a TAP-method that was previously used to isolate proteins associated with ligand-binding defective TR α 1 and TR β 1 mutants from HeLa cells (33), and improved on the method by i. using wt TR α 1 as bait, which allowed us to compare interactomes of liganded

and unliganded receptors, ii. instead of first separating proteins by SDS-PAGE and proteins subjecting the final eluate directly to LC-MS/MS to identify all proteins irrespective of their visualization on an SDS-PAGE gel, and iii. replicating the purifications for each condition to minimize the number of false positive hits. Our profiles partially overlap with the study of Fozzatti and coworkers, but returned a larger number of proteins that associate with TR α 1. For example, their study only returned CHD4, but we also found several additional proteins of the NuRD complex.

Our method was further validated by the recovery and co-immunoprecipitation of several known transcriptional co-regulators of TRs, such as RXR isoforms, the NCoR/SMRT corepressor complex in the absence of T3 and the Mediator and RNA polymerase II complexes in the presence of T3 (Table 3). Furthermore, the fact that we found many if not most subunits for these complexes shows that our method not only finds binary binding partners, but is mild and sensitive enough to preserve the complexes and identify indirect binding partners of TR α 1. This is for example demonstrated by the fact that from the RNA polymerase complex II, which only associates with TR α 1 via the large multisubunit Mediator complex, we also identified the regulatory kinase CDK9 (34) and phosphatase RPAP2 (35). One exception were the NCoA/SRC coactivator complexes, which were underrepresented in our purifications. We found NCoA1/SRC1 and NCoA3/SRC3 only in one HepG2 purification in the presence of T3 (Supplementary Table 1 (14)) and did not detect any HAT proteins. Co-immunoprecipitations, however, showed T3-dependent binding of SRC1 in both HepG2 and SH-SY5Y cells (Figure 4). Most likely, the SRC1 binding is sensitive to the prolonged purification procedure of the tandem versus the single affinity purification method.

In conclusion, we successfully and efficiently purified cell-type and ligand state specific TR α 1-interactomes using a simple tandem-affinity purification method and identified potentially novel interactions with signalling proteins, transcriptional regulators and chromatin remodelling complexes. Future studies will need to elucidate how these novel binding partners contribute to TR α 1-mediated gene regulation by TH and how specific mutations in TR α 1 affect the repertoire of recruited cofactors and downstream gene regulation, and ultimately the RTHa phenotype in patients.

Acknowledgements

During the course of this work, our mentor and friend professor Theo J. Visser sadly passed away and has therefore not been able to approve the final version of this manuscript. We thank Theo deeply for his contributions.

Grants and funding

This work was supported by ZonMW TOP Grant 91212044 and an Erasmus MC Medical Research Advisory Committee (MRACE) grant (RPP, MEM, WEV), Chiang Mai University (KW), and ZonMW Grant 91113020 for financial support for the MS infrastructure and the research programme Open Technology from the Netherlands Organisation for Scientific Research (NWO), project number 12778 (TML, LJMD, LZ).

Disclosure statement

The authors have nothing to disclose

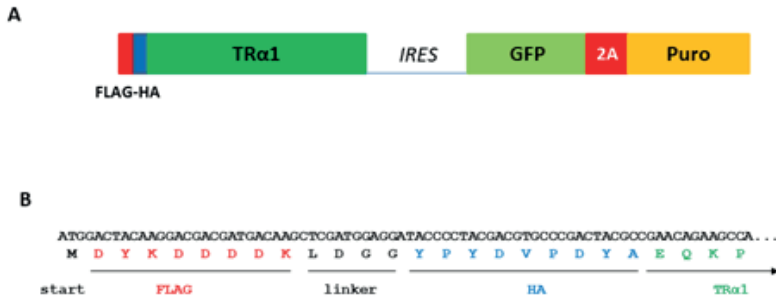
References

1. Cheng SY, Leonard JL, Davis PJ. Molecular aspects of thyroid hormone actions. *Endocr Rev.* 2010;**31**(2):139-170.
2. Brent GA. Mechanisms of thyroid hormone action. *J Clin Invest.* 2012;**122**(9):3035-3043.
3. van Gucht ALM, Moran C, Meima ME, Visser WE, Chatterjee K, Visser TJ, Peeters RP. Resistance to Thyroid Hormone due to Heterozygous Mutations in Thyroid Hormone Receptor Alpha. *Curr Top Dev Biol.* 2017;**125**:337-355.
4. Nagy L, Schwabe JW. Mechanism of the nuclear receptor molecular switch. *Trends Biochem Sci.* 2004;**29**(6):317-324.
5. Fondell JD, Ge H, Roeder RG. Ligand induction of a transcriptionally active thyroid hormone receptor coactivator complex. *Proc Natl Acad Sci U S A.* 1996;**93**(16):8329-8333.
6. Fondell JD. The Mediator complex in thyroid hormone receptor action. *Biochim Biophys Acta.* 2013;**1830**(7):3867-3875.
7. Allen BL, Taatjes DJ. The Mediator complex: a central integrator of transcription. *Nat Rev Mol Cell Biol.* 2015;**16**(3):155-166.
8. Lee JW, Choi HS, Gyuris J, Brent R, Moore DD. Two classes of proteins dependent on either the presence or absence of thyroid hormone for interaction with the thyroid hormone receptor. *Mol Endocrinol.* 1995;**9**(2):243-254.
9. Yap N, Yu CL, Cheng SY. Modulation of the transcriptional activity of thyroid hormone receptors by the tumor suppressor p53. *Proc Natl Acad Sci U S A.* 1996;**93**(9):4273-4277.
10. Wei LN, Hu X. Receptor interacting protein 140 as a thyroid hormone-dependent, negative co-regulator for the induction of cellular retinoic acid binding protein I gene. *Mol Cell Endocrinol.* 2004;**218**(1-2):39-48.
11. Hahm JB, Schroeder AC, Privalsky ML. The two major isoforms of thyroid hormone receptor, TRalpha1 and TRbeta1, preferentially partner with distinct panels of auxiliary proteins. *Mol Cell Endocrinol.* 2014;**383**(1-2):80-95.
12. Fozzatti L, Lu C, Kim DW, Cheng SY. Differential recruitment of nuclear coregulators directs the isoform-dependent action of mutant thyroid hormone receptors. *Mol Endocrinol.* 2011;**25**(6):908-921.
13. van Gucht AL, Meima ME, Zwaveling-Soonawala N, Visser WE, Fliers E, Wennink JM, Henny C, Visser TJ, Peeters RP, van Trotsenburg AS. Resistance to Thyroid Hormone Alpha in an 18-Month-Old Girl: Clinical, Therapeutic, and Molecular Characteristics. *Thyroid.* 2016;**26**(3):338-346.
14. Meima ME, Wejaphikul K, Leeuwenburgh S, Van Gucht ALM, Zeneyedpour L, Dekker LJM, Visser WE, Luider TM, Peeters RP. HUMAN LIVER AND NEURONAL INTERACTOMES REVEAL NOVEL BINDING PARTNERS FOR THE T3-RECEPTOR ISOFORM α 1. *Erasmus MC Digital Repository 2019.* 2019; **Deposited 2 May 2019**(<http://hdl.handle.net/1765/116349>).
15. van Mullem AA, Chrysis D, Eythimiadou A, Chroni E, Tsatsoulis A, de Rijke YB, Visser WE, Visser TJ, Peeters RP. Clinical phenotype of a new type of thyroid hormone resistance caused by a mutation of the TRalpha1 receptor: consequences of LT4 treatment. *J Clin Endocrinol Metab.* 2013;**98**(7):3029-3038.
16. Denslow SA, Wade PA. The human Mi-2/NuRD complex and gene regulation. *Oncogene.* 2007;**26**(37):5433-5438.
17. Xue Y, Wong J, Moreno GT, Young MK, Cote J, Wang W. NURD, a novel complex with both ATP-dependent chromatin-remodeling and histone deacetylase activities. *Mol Cell.* 1998;**2**(6):851-861.
18. Johnson DR, Lovett JM, Hirsch M, Xia F, Chen JD. NuRD complex component Mi-2beta binds to and represses RORgamma-mediated transcriptional activation. *Biochem Biophys Res Commun.* 2004;**318**(3):714-718.
19. Sokpor G, Xie Y, Rosenbusch J, Tuoc T. Chromatin Remodeling BAF (SWI/SNF) Complexes in

- Neural Development and Disorders. *Front Mol Neurosci.* 2017;**10**:243.
20. Wilson BG, Roberts CW. SWI/SNF nucleosome remodellers and cancer. *Nat Rev Cancer.* 2011;**11**(7):481-492.
 21. Huang ZQ, Li J, Sachs LM, Cole PA, Wong J. A role for cofactor-cofactor and cofactor-histone interactions in targeting p300, SWI/SNF and Mediator for transcription. *EMBO J.* 2003;**22**(9):2146-2155.
 22. Miyake N, Koshimizu E, Okamoto N, Mizuno S, Ogata T, Nagai T, Kosho T, Ohashi H, Kato M, Sasaki G, Mabe H, Watanabe Y, Yoshino M, Matsuishi T, Takanashi J, Shotelersuk V, Tekin M, Ochi N, Kubota M, Ito N, Ihara K, Hara T, Tonoki H, Ohta T, Saito K, Matsuo M, Urano M, Enokizono T, Sato A, Tanaka H, Ogawa A, Fujita T, Hiraki Y, Kitanaka S, Matsubara Y, Makita T, Taguri M, Nakashima M, Tsurusaki Y, Saito H, Yoshiura K, Matsumoto N, Niikawa N. MLL2 and KDM6A mutations in patients with Kabuki syndrome. *Am J Med Genet A.* 2013;**161A**(9):2234-2243.
 23. Hong YK, Detmar M. Prox1, master regulator of the lymphatic vasculature phenotype. *Cell Tissue Res.* 2003;**314**(1):85-92.
 24. Stergiopoulos A, Elkouris M, Politis PK. Prospero-related homeobox 1 (Prox1) at the crossroads of diverse pathways during adult neural fate specification. *Front Cell Neurosci.* 2014;**8**:454.
 25. Stein S, Oosterveer MH, Matak C, Xu P, Lemos V, Havinga R, Dittner C, Ryu D, Menzies KJ, Wang X, Perino A, Houten SM, Melchior F, Schoonjans K. SUMOylation-dependent LRH-1/PROX1 interaction promotes atherosclerosis by decreasing hepatic reverse cholesterol transport. *Cell Metab.* 2014;**20**(4):603-613.
 26. Lee S, Kang J, Yoo J, Ganesan SK, Cook SC, Aguilar B, Ramu S, Lee J, Hong YK. Prox1 physically and functionally interacts with COUP-TFII to specify lymphatic endothelial cell fate. *Blood.* 2009;**113**(8):1856-1859.
 27. Song KH, Li T, Chiang JY. A Prospero-related homeodomain protein is a novel co-regulator of hepatocyte nuclear factor 4alpha that regulates the cholesterol 7alpha-hydroxylase gene. *J Biol Chem.* 2006;**281**(15):10081-10088.
 28. Qin J, Gao DM, Jiang QF, Zhou Q, Kong YY, Wang Y, Xie YH. Prospero-related homeobox (Prox1) is a corepressor of human liver receptor homolog-1 and suppresses the transcription of the cholesterol 7-alpha-hydroxylase gene. *Mol Endocrinol.* 2004;**18**(10):2424-2439.
 29. Takeda Y, Jetten AM. Prospero-related homeobox 1 (Prox1) functions as a novel modulator of retinoic acid-related orphan receptors alpha- and gamma-mediated transactivation. *Nucleic Acids Res.* 2013;**41**(14):6992-7008.
 30. Broekema MF, Hollman DAA, Koppen A, van den Ham HJ, Melchers D, Pijnenburg D, Ruijtenbeek R, van Mil SWC, Houtman R, Kalkhoven E. Profiling of 3696 Nuclear Receptor-Coregulator Interactions: A Resource for Biological and Clinical Discovery. *Endocrinology.* 2018;**159**(6):2397-2407.
 31. Kamiya A, Kakinuma S, Onodera M, Miyajima A, Nakauchi H. Prospero-related homeobox 1 and liver receptor homolog 1 coordinately regulate long-term proliferation of murine fetal hepatoblasts. *Hepatology.* 2008;**48**(1):252-264.
 32. Sinha RA, Singh BK, Yen PM. Direct effects of thyroid hormones on hepatic lipid metabolism. *Nat Rev Endocrinol.* 2018;**14**(5):259-269.
 33. Fozzatti L, Kim DW, Park JW, Willingham MC, Hollenberg AN, Cheng SY. Nuclear receptor corepressor (NCOR1) regulates in vivo actions of a mutated thyroid hormone receptor alpha. *Proc Natl Acad Sci U S A.* 2013;**110**(19):7850-7855.
 34. Ramanathan Y, Rajpara SM, Reza SM, Lees E, Shuman S, Mathews MB, Pe'ery T. Three RNA polymerase II carboxyl-terminal domain kinases display distinct substrate preferences. *J Biol Chem.* 2001;**276**(14):10913-10920.
 35. Egloff S, Zaborowska J, Laitem C, Kiss T, Murphy S. Ser7 phosphorylation of the CTD recruits the RPAP2 Ser5 phosphatase to snRNA genes. *Mol Cell.* 2012;**45**(1):111-122.

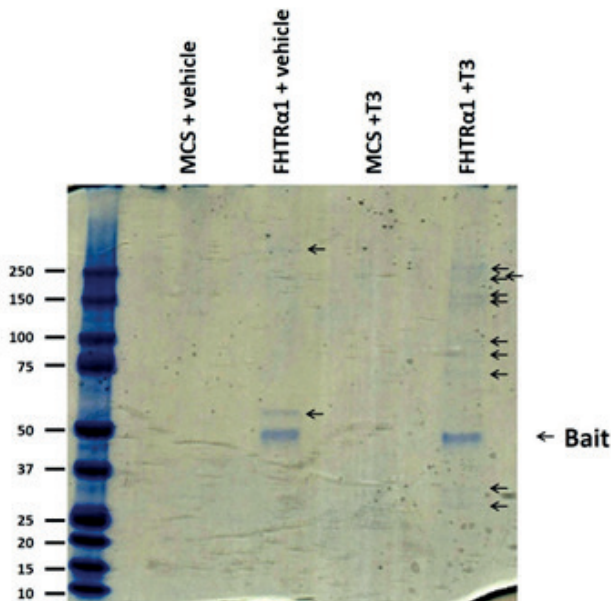
Supplementary Materials

Supplementary Figures

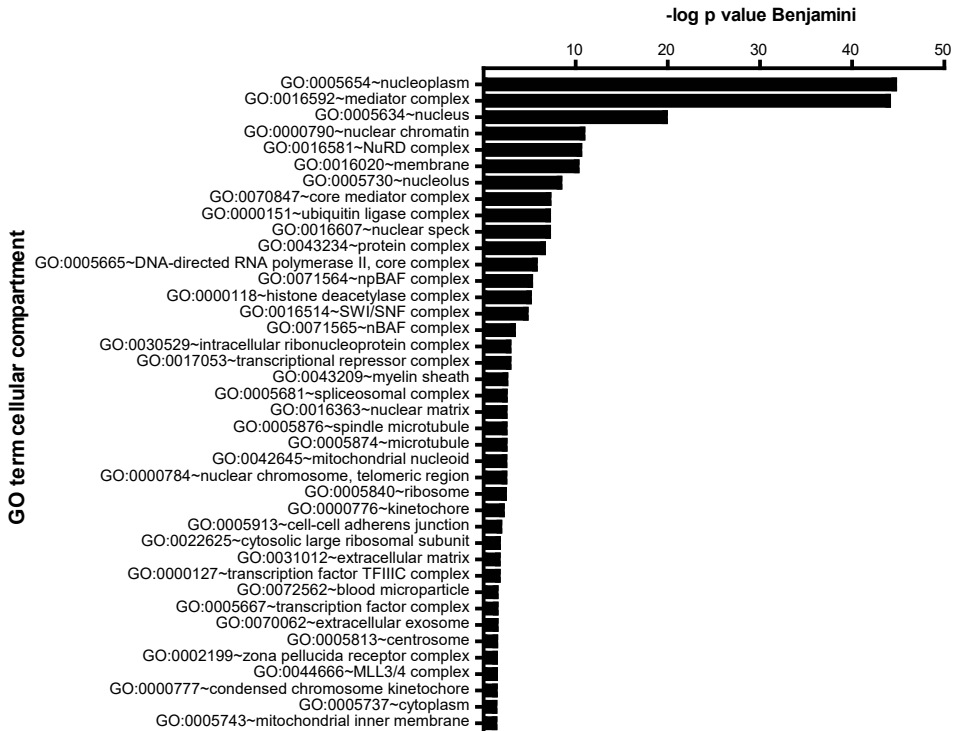


Supplementary Figure S1. Structure of expression cassette of the FLAG-HA tagged TR α 1 (FHTR α 1) construct. The second codon of the full length coding sequence of TR α 1 is fused at the 5'-end to consecutive sequences encoding the FLAG and hemagglutinin (HA) epitope tags (B). To select cells expressing FHTR α 1, the construct is expressed from a bicistronic messenger RNA, due to the inclusion of an internal ribosome entry site (IRES) sequence, together with a selection marker consisting of the sequences encoding the puromycine resistance gene (PURO) and green fluorescent protein (GFP), fused by the sequence encoding the 2A self-cleaving peptide (A).

6



Supplementary Figure S2. SDS-PAGE of FHTR α 1-containing protein complexes from HepG2 cells. HepG2 cells expressing FHTR α 1 or empty vector (MCS) as control were stimulated for 4 hrs with vehicle or 100 nM T3 and subjected to TAP purifications. One third of the final eluates were separated on a 4-12% Bis-Tris gel and protein bands visualized by Colloidal Coomassie staining.



Supplementary Figure S3. Enrichment for cellular compartments of the total profile. Proteins that specifically co-purified with FHTRα1 in any purification (Supplementary Table 1) were analysed for enrichment of cellular compartment using DAVID (minimum count 2, ease 0.1). The top 40 most significant GO terms are displayed. P values were adjusted for false discovery rates using the Benjamini correction.

Supplementary Methods

Construction of lentiviral vectors pWCAGpCasC-MCS-IRESpuro2AGFP and pWCAGpCasC-FHTR α 1-IRESpuro2AGFP

To add the sequence encoding the FLAG and HA epitope to the 5'-side of TR α 1, the full length coding sequence for TR α 1 was amplified using Pfu polymerase (Thermofisher) by which the start codon was replaced with consecutive sequences for the FLAG and HA epitope tag (Supplementary Figure S1). The resulting fragments was cloned into the pCR2.1TOPO vector (Invitrogen) and subsequently excised and ligated into the HindIII and BamHI sites of pENTL1-MCS-R5 to yield the plasmid pENTL1-FHTR α 1-R5. The correct sequence was confirmed by Sanger sequencing. The MCS (multiple cloning site) or FHTR α 1 fragments were next fused to the IRESpuro2AGFP-fragment from pENTL5-IRESpuro2AGFP-R2 and inserted into pWCAGpCasC by multiple gateway cloning using the LR II Clonase Plus (Invitrogen) according to the manufacturers protocol.

Tandem affinity purification

Throughout the procedure, buffers were supplemented with 100 nM T3 or vehicle, and cOmpleteTM protease inhibitors cocktail (Roche). Cells were washed twice with ice-cold DPBS, scraped into 2 ml DPBS per plate, pelleted in a table-top centrifuge at 1200 round per minute (rpm) for 5 minutes at 4 °C and resuspended in 5 ml buffer A (10 mM Hepes.NaOH, 10 mM KCl, 0.1 mM EDTA, 1 mM DTT, pH 7.9). After 15 min on ice, 0.6% NP40 was added and the cells were vortexed for 30 seconds to lyse the cells. Phosphatase inhibitors (5 mM NaF and 1 mM NaPPi) were added and nuclei pelleted by centrifugation at 2000 rpm for 10 minutes at 4 °C. Nuclear proteins were extracted by nutating the nuclei in 1.88 ml buffer C (20 mM HEPES.NaOH, 400 mM NaCl, 1 mM EDTA, 1 mM DTT, 5 mM NaF, 1 mM NaPPi, pH 7.9) for 20 minutes at 4 °C. The nuclei were spun down in a microfuge at 15000 rpm. The supernatant was transferred to a 15 ml conical tube, the salt concentration reduced by addition of 3.12 ml buffer D (20 mM HEPES.NaOH, 1 mM EDTA, 5 mM NaF, 1 mM NaPPi, pH 7.9) and NP40 added to a final concentration of 0.1%. Next, FHTR α 1-containing protein complexes were bound overnight at 4 °C to 20 μ l bedvolume of anti-FLAG agarose (clone M2; Sigma), washed 1 time with 10 ml and 4 times with 1 ml of ice-cold washbuffer (20 mM HEPES.NaOH, 150 mM NaCl, 1 mM EDTA, 5 mM NaF, 1 mM NaPPi, 0.1% NP40, pH 7.9) and eluted twice with 50 μ l of 200 μ g/ml FLAG peptide (Sigma) in washbuffer for 30' at 4 °C in spin columns (Biorad). Eluates were combined, 500 μ l of washbuffer was added to the eluates and FHTR α 1-containing protein complexes were bound overnight at 4 °C to 20 μ l bedvolume of anti-HA agarose (Sigma), after which the resin was washed 4 times with 1 ml ice-cold washbuffer. For the first purification from HepG2 cells, the resin was subsequently washed 1 time with 1 ml washbuffer without NP40, transferred into a spin column and protein complexes eluted once at 4 °C and once at room temperature with 25 μ l 400 μ g/ml HA peptide (Sigma), after which the eluates were pooled. For the other purifications, 0.1% RapiFest SF (Waters)

was added to the final washbuffer and elution buffer, to improve bead handling. Elutes were pooled and subjected to LC-MS/MS for protein identification. For the first purification from HepG2 cells, 1/3 part of the eluate was denatured in 1x NuPAGE LDS sample buffer (Thermo Fisher Scientific) supplemented with 10 mM DTT at 70 °C for 10 minutes, separated by SDS-PAGE on a 4-12% Bis-Tris gel (Novex, Invitrogen) and bands visualized with a Colloidal Blue Staining Kit (Invitrogen).

In-solution digestion

Eluates from two independent purifications from each cell line were precipitated using acetone and then resuspended in 0.1% Rapigest in 50 mM NH_4HCO_3 . The solution was reduced with 100 mM dithiothreitol (DTT) at 60 °C for 30 minutes. After the mixture was cooled down to room temperature, it was alkylated in the dark with 300 mM iodoacetamide at ambient temperature for 30 minutes, and digested overnight with 0.4 μg trypsin (Promega, Madison, WI). Five percent trifluoroacetic acid was added, to obtain a final concentration of 0.5% trifluoroacetic acid ($\text{pH} < 2$). After 45 minutes of incubation at 37 °C, the samples were centrifuged at 13,000 x g for 10 minutes.

NanoLC data dependent mass spectrometry measurements

Digested samples were subjected to LC-MS/MS analysis. Samples were analyzed by nano-LC (Ultimate 3000RS, Thermo Fisher Scientific, Germering, Germany). After pre-concentration and washing of the samples on a C18 trap column (1 mm \times 300 μm i.d., Thermo Fisher Scientific), they were loaded onto a C18 column (PepMap C18, 75 mm ID \times 150 mm, 2 μm particle and 100 Å pore size, Thermo Fisher Scientific) using a linear 15 minutes gradient (4-38% ACN/H₂O; 0.1% formic acid) at a flow rate of 250 nL/min. The separation of the peptides was monitored by a UV detector (absorption at 214 nm). The integrated area of the UV chromatogram is used to determine the maximum injection volumes for the LC-MS analyses. For the LC-MS the same type of LC system is used connected to a nanospray source. The LC system was equipped with a PepMap C18 column (75 mm ID \times 250 mm, 2 μm particle and 100 Å pore size, Thermo Fisher Scientific) and a 30 or 90 minutes gradient (4-38% ACN/H₂O; 0.1% formic acid) at a flow rate of 300 nL/min coupled to either an Orbitrap Fusion or to a Orbitrap Fusion Lumos (Thermo Fisher Scientific, San Jose, CA, USA). The Orbitrap Fusion Lumos was operated in the data dependent acquisition (DDA) mode. Full scan MS spectra (m/z 375-1,500) in profile mode were acquired in the orbitrap with a resolution of 120,000 after accumulation of an AGC target of 400,000. A top speed method with a maximum duty cycle of 3 seconds was used. In these 3 seconds, the most intense peptide ions from the full scan in the orbitrap were fragmented by HCD (normalized collision energy 28%) and measured in the iontrap with a AGC target of 10,000. Maximum fill times were 50 ms for the full scans and 50 ms for the MS/MS scans. Precursor ion charge state screening was enabled and only charge states from 2-7 were selected for fragmentation. The dynamic exclusion was activated after the first time a precursor was selected for fragmentation and excluded for a

period of 60 seconds using a relative mass window of 10 ppm. Lock mass correction was activated to improve mass accuracy of the survey scan. In the Orbitrap Fusion the following settings were used; DDA mode, Full scan MS spectra (m/z 400-1,600) in profile mode with a resolution of 120,000 and an AGC target of 400,000. A top speed method with a maximum duty cycle of 3 seconds was used. In these 3 seconds, the most intense peptide ions from the full scan in the orbitrap were fragmented by CID (normalized collision energy 30%) and measured in the iontrap with a AGC target of 10,000. Maximum fill times were 100 ms for the full scans and 40 ms for the MS/MS scans. The rest of settings were the same as for the measurements on the Orbitrap Fusion Lumos. From the data files of both systems the MS/MS spectra were extracted and converted into mgf files by using MSConvert of ProteoWizard (version 3.0.06245). All mgf files were analyzed using Mascot (version 2.3.02; Matrix Science, London, UK). Mascot was used to perform database searches against the human subset of either uniprot_sprot download November 2015 (20194 entries) or download September 2014 (20196 entries), using Mascot version 2.3.02. Monoisotopic fragment tolerance was set to 0.50 Da and parental tolerance at 10 ppm. Carbamidomethylation of cysteine was specified as fixed modification and oxidation of methionine as variable modification for all, and n-terminal acetylation for the first HepG2 purification.

Version 4.8.3 of the Scaffold platform was used to validate proteins and peptides. Stringency settings allowed FDRs of 1% for proteins and peptides when screened against a decoy database. This allowed probability scores of 5% and 78% for proteins and peptides respectively with a minimum of 2 peptides for the first purification from HepG2, and 99% and 91% for proteins and peptides with a minimum of 1 peptide for the other purification. Proteins that were present in any of the control purifications were excluded from our final profile. The uniprot_sprot database contains the TR α isoform 2 (P10827-1) instead of our bait TR α 1 (P10827-2). These isoforms differ in their C-terminal domain (371-410 in TR α 1), which has high homology between TR α 1 and TR β . Therefore, a peptide (sequence MIGACHASR; position 376-384 in TR α 1, position 440-448 in TR β 1) that is conserved between TR α 1 and TR β was scored as an exclusive unique peptide for the C-terminus of TR β . Apart from one peptide with a probability score of 85% (sequence KLIEENR; position 190-196 in TR β 1), in HepG2 purification 1 from vehicle treated cells, we did not find any peptides that are unique for TR β as well as TR α 2. As such, we decided that all peptides are derived from TR α 1 and assigned the C-terminal peptide and spectra to TR α 1 in Table 2 and Supplementary Table 1. Gene enrichment analysis was performed using the Database for Annotation, Visualization and Integrated Discovery (DAVID), version 6.8 (<https://david.ncifcrf.gov/>) using default settings (count 2, ease 0.1) and p-values adjusted using the Benjamini correction. Existing protein interaction networks were searched using STRINGS (<https://strings-db.org>) with minimum required interaction scores set at medium confidence (0.400).

